IJIE

UTHM Penerbit
Universiti Tun Hussein Onn Malaysia

INTERNATIONAL JOURNAL OF INTEGRATED ENGINEERING
ISSN: 2229-838X e-ISSN: 2600-7916

Vol. 18 No. 2 (2026) 195-212
https://publisher.uthm.edu.my/ojs/index.php/ijie

Performance Evaluation of Iris Diffuser Dampers in HVAC: Systems Using CFD Analysis

Nur'Amirah Busu[1], Norasikin Mat Isa[1]*, Mohamed Hussein[2], Azian Hariri[1], David Shina Adebayo[3], M.F. Abdul Ghani[1,4]

[1] *Faculty of Mechanical and Manufacturing Engineering, Universiti Tun Hussein Onn Malaysia, Parit Raja, Johor, 86400, MALAYSIA*

[2] *Faculty of Mechanical Engineering, Universiti Teknologi Malaysia, Skudai, Johor, 81310, MALAYSIA*

[3] *School of Engineering and Technology, College of Engineering and Physical Sciences, Aston University, Aston Triangle, Birmingham B4 7ET, UNITED KINGDOM*

[4] *Acson Malaysia Sales and Service Sdn. Bhd., No 7A, Jalan 13/4, Seksyen 13, Petaling Jaya, Selangor, 46200, MALAYSIA*

*Corresponding Author: sikin@uthm.edu.my
DOI: https://doi.org/10.30880/ijie.2026.18.02.016

Article Info

Received: 15 November 2025
Accepted: 20 March 2026
Available online: 28 April 2026

Keywords

Diffuser damper, Iris damper, performance evaluation, thermal comfort, VWA analysis, contour analysis, CFD simulation, ANSYS Fluent, HVAC

Abstract

Air distribution in HVAC systems plays a critical role in ensuring indoor thermal comfort and energy efficiency, yet the impact of diffuser damper design on airflow and temperature regulation is often overlooked. This study investigates the performance of three diffuser damper designs, Iris, Butterfly, and Radial under varying opening conditions, addressing the need for precise airflow control and optimized thermal distribution in indoor environments. CFD simulations were conducted using ANSYS Fluent, employing a realizable k–ε turbulence model to evaluate flow and thermal characteristics. Six key parameters; static temperature, velocity magnitude, static pressure, turbulent kinetic energy, turbulent intensity, and turbulent dissipation rate; were analysed using volume-weighted averages across the computational domain to provide a comprehensive performance assessment. Results indicated that the Iris damper consistently achieved precise temperature regulation, lower turbulence, and smoother airflow across all opening conditions, making it ideal for applications requiring stable thermal comfort and energy efficiency. The Butterfly design offered balanced performance suitable for general comfort applications, while the Radial design, despite achieving high airflow velocities, generated elevated turbulence at restricted openings, limiting its suitability for precision-controlled environments. In conclusion, the Iris damper emerged as the optimal configuration for enhancing indoor thermal comfort and optimizing HVAC system performance across diverse operational scenarios.

1. Introduction

Maintaining optimal thermal comfort in indoor environments is increasingly vital, given that occupants spend over 90% of their time indoors. Heating, Ventilation, and Air Conditioning (HVAC) systems constitute one of the most critical infrastructures in contemporary buildings, contributing nearly half of the overall energy consumption in both residential and commercial sectors [1]. In HVAC systems, air diffusers are the visible end devices that deliver conditioned air into occupied zones, where diffuser geometry, placement, and discharge pattern have been widely studied as the main determinants of thermal comfort and energy performance. Recent research on diffuser performance and HVAC optimization demonstrates diverse approaches ranging from diffuser blade geometry to adaptive control strategies.

For instance, Jeffrey [2] focused on round ceiling diffusers with varying blade numbers (4, 5, and 7 blades), anticipating that more blades would enhance airflow uniformity and thermal distribution. Meanwhile another investigation by Essam et al. [3] examined square four-way diffusers in a classroom and emphasized the importance of air discharge angle and velocity, with findings validated through both CFD and experimental data. Similarly, previous researchers [4], [5], applied CFD to hospital operating rooms, focusing on air distribution for both thermal comfort and contaminant control, reflecting the importance of diffuser design in critical healthcare environments. Meanwhile, Joanna et al. [6] emphasized acoustic performance, analyzing noise reduction in swirl diffusers with serrated blades, which adds another dimension often overlooked in airflow and comfort studies. Mengchao et al. [7] further contributed by optimizing swirl diffuser shapes using a comprehensive evaluation index applicable across both winter and summer, addressing seasonal adaptability.

Unlike these geometry-based studies, Linye et al. [8] critiqued the limitations of traditional constant velocity (CMV) control in variable air volume (VAV) systems and proposed a constant jet throw length (CMT) method, achieving substantial improvements in airflow diffusion performance. Meanwhile, Dong and Seongju [9] shifted attention from diffuser design to system integration, showing that a smart window-integrated ventilation (SWV) system could complement centralized HVAC to improve indoor air quality and comfort, though its effectiveness varied seasonally. Extending further, Farrokh et al. [10] introduced human-aware adaptive operations with active diffusers, demonstrating that coupling occupant feedback with directional airflow control could improve comfort and reduce energy demand by approximately 25%. Collectively, these studies highlight that while diffuser geometry remains fundamental for airflow distribution, adaptive and hybrid systems offer significant potential for dynamic optimization.

However, one critical but often overlooked component is the diffuser damper, a flow-regulating device installed directly above the diffuser outlet. Unlike VAV dampers which located in VAV boxes upstream in duct branches and widely reported in the literature [11]-[18], diffuser dampers are rarely acknowledged in both research and building practice. In fact, most buildings omit diffuser dampers entirely, largely due to cost-saving strategies during installation. Instead, airflow regulation is typically achieved only through diffuser design or upstream duct dampers. As a result, the specific role of diffuser dampers in modulating near-diffuser airflow, temperature stratification, turbulence, and energy efficiency has received limited scholarly attention.

This study aims to highlight the often-overlooked existence and significance of diffuser dampers by demonstrating their influence through a comparative CFD investigation under various opening conditions. Currently, all diffuser dampers in practice are limited to manual adjustment, with no motorized variant available to enable adaptive control. To address this gap, the present work explores the potential of the Iris diffuser damper design, comparing it with the existing manual configuration to evaluate its capability in optimizing indoor temperature distribution. Using volume-weighted average (VWA) parameters, namely static temperature, velocity magnitude, static pressure, turbulent kinetic energy (TKE), turbulence intensity (TI), and turbulent dissipation rate (ε). This study establishes a comprehensive evaluation framework that extends beyond localized point measurements. This domain-wide analysis offers new insights into the underexplored role of diffuser dampers in enhancing indoor thermal comfort and advancing HVAC performance research. Relevant prior research connected to this study can be found in [19], [20]-[23].

2. Methodology

This study employed Computational Fluid Dynamics (CFD) simulations using ANSYS Fluent to evaluate the performance of three diffuser damper designs which were Iris, Butterfly, and Radial, under varying opening conditions as in Table 1.

Table 1 *The damper designs and opening conditions*

	Damper design	 Iris	 Butterfly	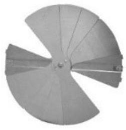 Radial
Opening condition	Maximum	360° (150 mm)	90°	288°
	Medium	65.45° (110 mm)	45°	180°
	Minimum	0° (80 mm)	25°	102°

2.1 The Modelling of Computational Domain

A chamber was modelled in ANSYS SpaceClaim to represent an indoor environment for the computational domain. The inner dimensions of the chamber were 5 ft × 5 ft × 4 ft (1.52 m × 1.52 m × 1.22 m) for length, width, and height, respectively, as illustrated in Fig. 1(a). The sizing was determined based on the laboratory-scaled test rig as in Fig. 1(b) which available in the EnRG Lab, Universiti Tun Hussein Onn Malaysia (UTHM), ensuring consistency between the numerical model and the experimental setup.

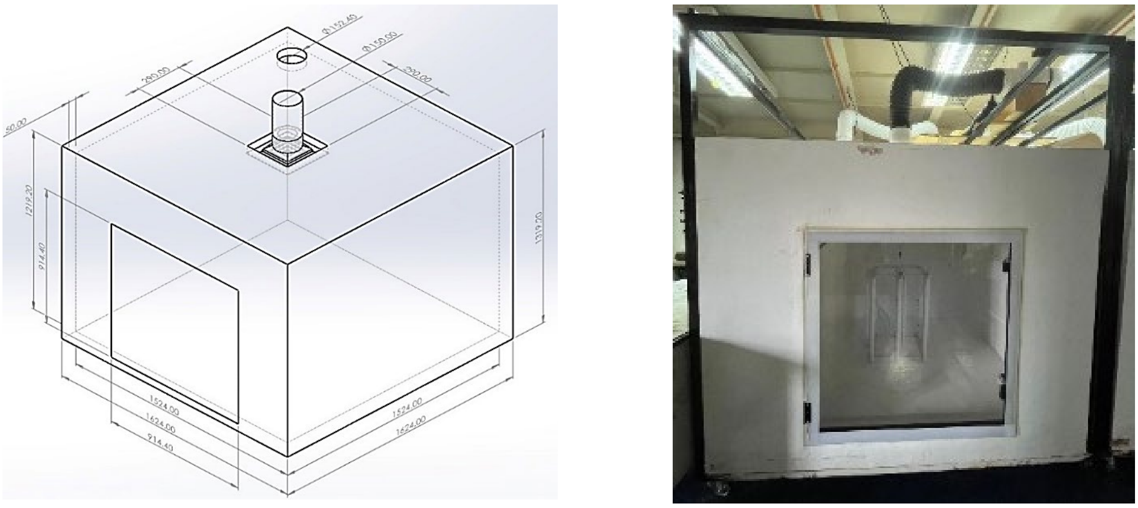

(a) **(b)**

Fig. 1 *(a) The dimension of lab-scaled test rig chamber; (b) The actual lab-scaled test rig*

Each damper design was first modeled in SolidWorks and then imported into ANSYS Fluent for simulation. Fig. 2 illustrates the computational domain of the damper in its minimum opening condition, positioned above the outlet diffuser as shown in Fig. 1(a). The computational domains for the medium and maximum opening conditions are presented in Fig. 3 and Fig. 4, respectively.

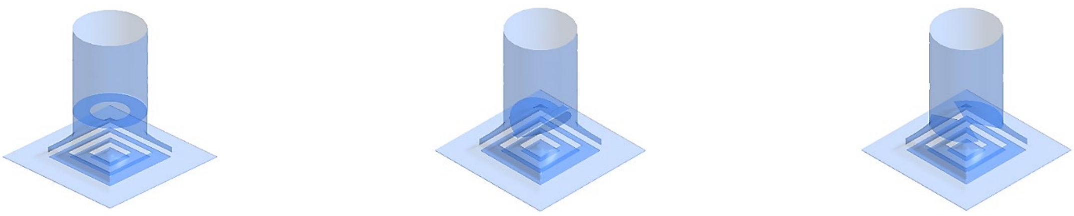

(a) **(b)** **(c)**

Fig. 2 *The damper's computational domain under minimum opening condition (a) Iris; (b) Butterfly; (c) Radial*

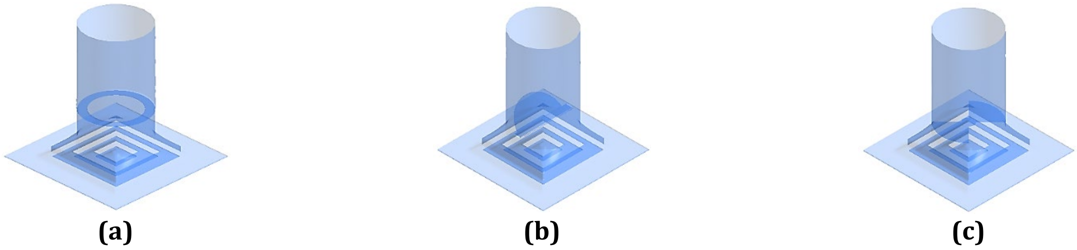

Fig. 3 *The damper's computational domain under medium opening condition (a) Iris; (b) Butterfly; (c) Radial*

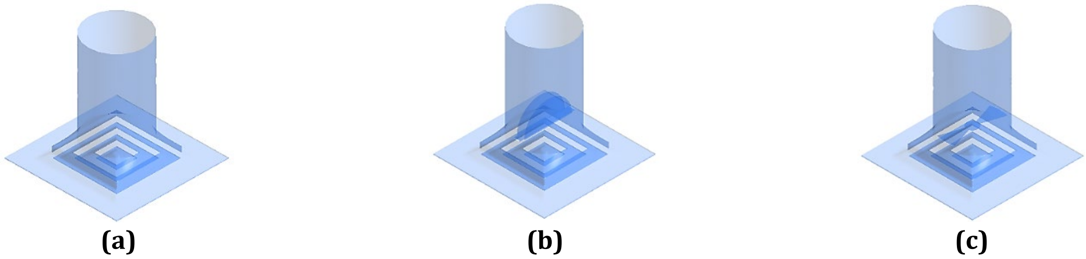

Fig. 4 *The damper's computational domain under maximum opening condition (a) Iris; (b) Butterfly; (c) Radial*

2.2 Mesh Generation

After defining the geometry, the meshing process was conducted using a tetrahedral unstructured grid to accommodate the complex geometry of the diffuser damper and surrounding duct. Six boundary surfaces were defined: inlet, outlet, duct, ceiling, wall, and floor, while the entire air domain was designated as Fluidzone to represent the computational region. Mesh defeaturing, curvature, and proximity settings in ANSYS were employed to refine the mesh and accurately resolve geometric and near-wall features. The resulting mesh of the fluid domain is illustrated in Fig. 5.

A grid independence test (GIT) was performed using a parameter set in ANSYS Fluent to ensure mesh quality and reliable simulation results. The body sizing element was selected as the input parameter, while the volume-averaged temperature, volume-averaged velocity, and maximum mesh skewness were monitored as output parameters. The element size was varied from 100 mm to 10 mm, and the results showed minimal variation beyond a certain refinement level, confirming grid-independent behavior.

For Iris damper with maximum opening condition, the trends of volume-averaged temperature, velocity, and maximum mesh skewness were evaluated across varying body sizing values. The temperature and velocity results remained nearly constant beyond 50 mm, indicating that further mesh refinement did not significantly affect the solution accuracy. Similarly, mesh skewness showed minimal variation between 50 mm and 100 mm, confirming sufficient mesh quality. Thus, the grid independence test determined an optimal body sizing of 55 mm. At this configuration, the mesh comprised 247,534 nodes and 1,356,206 elements. The maximum skewness of 0.799 and orthogonal quality of 0.201 indicated a mesh of acceptable quality within the recommended CFD range, ensuring numerical stability and accuracy.

Furthermore, the selected mesh achieved a good balance between resolution and computational efficiency, confirming that further refinement would not significantly affect the simulation results. It is important to note that the GIT was performed independently for every damper design, recognizing that each geometry produces distinct flow structures and mesh sensitivities. This approach ensures that the selected mesh size for each model is both accurate and physically representative.

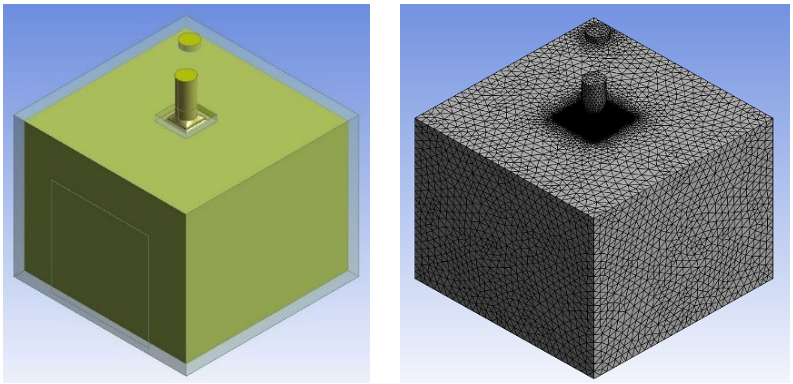

(a) (b)

Fig. 5 *(a) The fluid domain; (b) The generated mesh on the fluid domain*

2.3 Airflow Model

The Reynolds number (Re) is a dimensionless parameter used to characterize fluid flow by comparing inertial and viscous forces, expressed as:

$$Re = \frac{\rho V d}{\mu} \quad (1)$$

where ρ is the air density (kg/m^3), V is the airflow velocity (m/s), d is the duct hydraulic diameter (m), and μ is the dynamic viscosity (kg/m·s). Based on Eq. (1), the Reynolds number for airflow in the duct was calculated as 9548, using air properties of $\rho = 1.204\ kg/m^3$, V = 1.0 m/s, d = 0.15 m, and $\mu = 1.825 \times 10^{-5}$ kg/m·s. Since this value exceeds 2300, the flow was classified as turbulent.

Accordingly, the Reynolds-averaged Navier–Stokes (RANS) equations with the realizable k–ε turbulence model were employed to simulate indoor airflow. The realizable k–ε turbulence model was selected for this study due to its improved ability to capture complex indoor airflow patterns involving recirculation, swirl, and separation, which are common in diffuser damper applications. Unlike the standard k–ε model, the realizable version introduces a refined formulation for turbulent viscosity and a new transport equation for the dissipation rate (ε), enhancing prediction accuracy for flows with strong curvature and rotation.

Although the RNG k–ε model offers improvements for rapidly strained flows, previous studies have shown that the realizable k–ε model generally provides more accurate results in predicting velocity and temperature distributions in indoor environments [10], [22], [24]-[26]. More advanced models such as SST k–ω or LES were not employed, as they require significantly higher computational resources without proportionate accuracy gains for steady-state HVAC simulations. Thus, the realizable k–ε model provides an effective balance between accuracy, robustness, and computational efficiency, making it well-suited for the present CFD investigation.

The scalable wall treatment was adopted to enhance near-wall prediction while maintaining computational efficiency. It provides a balanced approach between the simplicity of the standard wall function and the precision of the enhanced treatment, making it suitable for complex geometries such as diffuser dampers and ducts.

2.4 Numerical Solution Method

The governing equations were solved using the pressure-based solver, with pressure–velocity coupling handled via the combination of SIMPLEC and Coupled algorithm. The two-stage solution strategy was applied to ensure computational efficiency and accuracy. The SIMPLEC scheme was first employed for the initial 300 iterations to achieve rapid convergence in the early phase. Subsequently, the simulation transitioned to the Coupled scheme to refine pressure–velocity coupling and improve overall solution stability. The use of pseudo-time stepping in the Coupled scheme further enhanced convergence smoothness and accuracy.

Second-order upwind discretisation was applied to the momentum, turbulence kinetic energy, and energy equations to enhance numerical accuracy. Convergence was determined when residuals fell below 10^{-5} for continuity, momentum, and turbulence equations, and below 10^{-6} for the energy equation. This hybrid approach effectively combined the efficiency of SIMPLEC with the robustness of the Coupled method, resulting in a well-converged and reliable CFD solution.

2.4.1 Boundary Conditions

The computational domain surfaces were assigned materials and physical properties to replicate realistic indoor conditions. The duct and damper were modelled using aluminium, while the ceiling, walls, and floor were assigned gypsum to represent common interior construction materials. All solid surfaces, including the duct, damper, ceiling, walls, and floor, were set as stationary walls, reflecting the absence of movement in the physical environment. A no-slip shear condition was applied to all walls to ensure that the airflow velocity at the wall boundaries was zero, consistent with standard indoor airflow modelling practices.

Surfaces with specified thermal interaction were assigned fixed temperatures, while others were treated with zero heat flux to represent adiabatic conditions. The numerical and thermal boundary conditions applied in the simulation are summarised in Table 2. All boundary conditions applied in the CFD simulations were defined to replicate the actual operating conditions of the laboratory test rig, ensuring that the numerical model accurately reflects the real experimental setup.

Table 2 *The numerical and thermal boundary conditions*

Boundary	Condition	Value
Velocity inlet	Velocity magnitude	1 m/s
	Turbulent intensity	8%
	Hydraulic diameter	0.15 m
	Temperature	18.0 °C
Pressure outlet	Gauge pressure	0 Pa
Ceiling	Temperature	27.0 °C
Walls	Temperature	28.5 °C
Floor	Heat flux	0

2.5 CFD Validation

To ensure simulation accuracy, validation was performed using the Iris damper with a 150 mm inlet aperture under an inlet velocity of 1 m/s and temperature of 18 °C. The experiment was conducted for 40 minutes, and the average temperature at the centre of test rig chamber was compared once both simulation and experiment reached steady-state conditions as shown in Fig. 6.

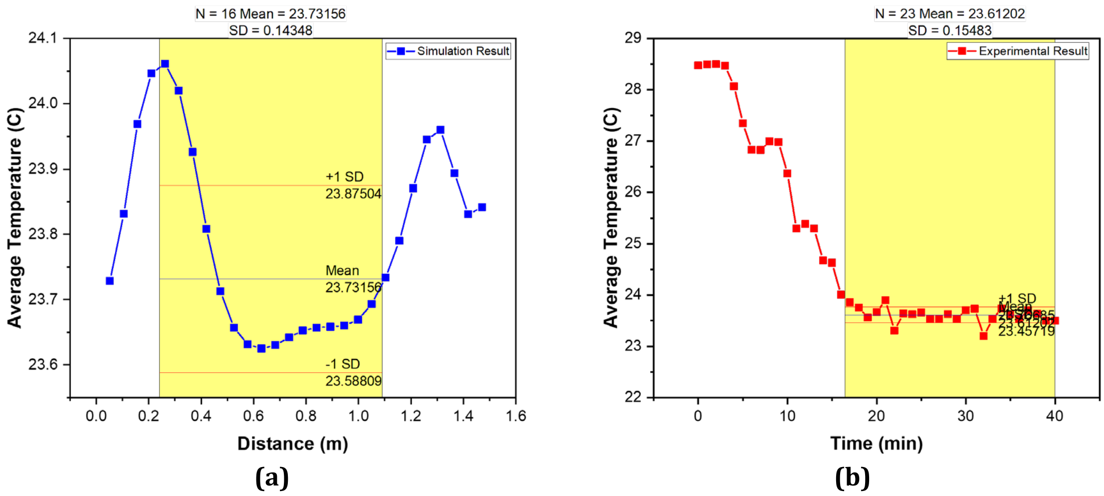

Fig. 6 *Validation of temperature profiles; (a) Simulation results; (b) Experimental measurements*

The validation data for the temperature profile, summarized in Table 3, show excellent agreement between the simulation (23.7 °C) and experimental (23.6 °C) mean temperatures, with a percentage deviation of only 0.507%. The difference in standard deviation between simulation (0.14 °C) and experiment (0.16 °C) was also minor, indicating consistent temperature fluctuation patterns. Overall, the CFD model demonstrated strong predictive capability for average indoor thermal conditions. Minor variations in standard deviation were attributed to differences in data sampling methods and did not significantly impact the validation outcome.

Table 3 *Summary of validation data*

Data type	Mean temperature (°C)	Percentage difference (%)	Standard deviation (°C)
Simulation	23.732	0.507	0.143
Experimental	23.612		0.155

2.6 Post-Processing

In this paper, the extracted data primarily focus on the performance evaluation based on volume-weighted average (VWA) analysis, followed by contour plot analysis as supporting evidence. The VWA analysis provides a reliable quantitative measure of the overall thermal and airflow performance across the entire computational domain, ensuring an objective comparison among damper designs. Meanwhile, the contour plots provide complementary qualitative visualization, illustrating the spatial variations in temperature and airflow that substantiate and enrich the interpretation of the VWA findings.

2.7 Volume-Weighted Average Analysis

The VWA analysis was used to evaluate and compare the overall performance of the diffuser damper designs. The VWA for any variable ϕ is calculated using:

$$VWA_{\emptyset} = \frac{\sum_{i=1}^{n} \emptyset_i V_i}{\sum_{i=1}^{n} V_i} \tag{2}$$

where ϕ_i is the value of the variable in each computational cell within the domain, and V_i is the corresponding cell volume. The averaging was performed over the entire computational domain to represent the overall airflow and thermal characteristics of the indoor space. This approach consolidates simulation results from all control volumes in the domain, providing a domain-wide representation rather than relying solely on point measurements.

Six VWA parameters were computed across the entire computational domain:

- Static Temperature (T)
- Velocity Magnitude (v)
- Static Pressure (P)
- Turbulent Kinetic Energy (k)
- Turbulent Intensity (TI)
- Turbulent Dissipation Rate (ε)

The VWA of static temperature (VWAT) represents the overall thermal condition of the space, where lower VWAT values in the occupied zone indicate enhanced cooling effectiveness, and uniform temperature fields suggest improved thermal comfort. The VWA of velocity magnitude (VWAv) reflects the overall airflow rate and mixing strength, with balanced velocities ensuring sufficient air circulation without inducing drafts, thereby contributing to both comfort and efficient air distribution. The VWA of static pressure (VWAP) provides insight into the flow resistance encountered across the damper, where lower pressure drops denote a more aerodynamically efficient design and reduced energy demand from the HVAC fan system.

Meanwhile, the turbulent parameters were computed using standard turbulence model equations:

$$k = \frac{1}{2}(u'^2 + v'^2 + w'^2) \tag{3}$$

$$TI = \frac{u'}{U} \times 100\% \tag{4}$$

$$\varepsilon = C_{\mu}^{3/4} \frac{k^{3/2}}{l} \tag{5}$$

where:

- u' , v' , w' are the fluctuating components of velocity in the x, y, and z directions,
- U is the mean velocity magnitude,
- C_μ is the turbulence model constant (typically 0.09), and
- l is the turbulence length scale.

The VWA of turbulent kinetic energy (VWAk) quantifies the intensity of velocity fluctuations, identifying regions of strong turbulence that promote mixing and thermal uniformity, although it may result in some pressure losses. The turbulent intensity (VWATI) further characterizes flow stability by relating velocity fluctuations to the mean velocity, where moderate levels indicate effective mixing, while excessively high values may lead to uneven air distribution or acoustic discomfort. Lastly, the turbulent dissipation rate (VWAε) describes the rate at which turbulent energy is converted into heat due to viscous effects, offering an understanding of turbulence decay and energy redistribution within the domain.

Together, these parameters establish an integrated evaluation framework for assessing diffuser damper performance with respect to airflow quality, thermal comfort, and energy efficiency. By consolidating simulation data across the entire computational domain, this approach enables a robust and accurate quantitative representation of the modelled environment. It provides a comprehensive assessment of thermal performance, airflow distribution, turbulence characteristics, and overall energy efficiency for each damper configuration.

2.7.1 Contour Plot Analysis

Contour plots are essential for identifying localized variations that may not be evident from averaged data, providing a clear visual interpretation of heat transfer and airflow uniformity. The temperature contour plot highlights the distribution of thermal gradients and regions of potential thermal stratification, while the velocity contour plot depicts flow paths and recirculation zones, offering valuable insights into the effect of airflow characteristics of each damper configuration in indoor space.

Fig. 7 illustrates the XY and YZ planes located at x = 0.762 m and z = 0.762 m, respectively, which were used to generate the two-dimensional temperature contours at the midsection of the fluid zone. The velocity contour was extracted along the mid-plane of the XZ section to capture the core airflow behaviour across the chamber.

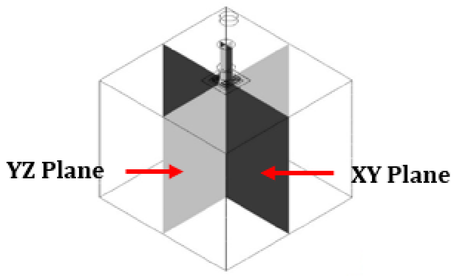

Fig. 7 *The position of XY and YZ planes in the chamber for temperature contour plot*

3. Results and Discussion

A comprehensive evaluation of the diffuser damper performance was conducted using VWA values of key flow and thermal parameters. A simulation analysis was performed to assess the performance of Iris, Butterfly, and Radial dampers in terms of temperature distribution and airflow characteristics within a closed chamber.

In addition to the quantitative assessment, contour plots were analyzed to illustrate the spatial distributions of temperature, velocity, and turbulence within the computational domain. This combined quantitative–qualitative approach enables both global and localized evaluation of diffuser damper behaviour, providing a thorough understanding of performance variations among different designs and opening conditions.

3.1 Volume-weighted Average Static Temperature (VWAT)

The first parameter evaluated was the VWAT, which provides an overall measure of the thermal energy within the computational domain. This parameter is particularly useful for assessing the effectiveness of a system in heating or cooling a space, as well as the uniformity of temperature distribution. Fig. 8 presents a comparison of the VWAT for three damper designs under maximum, medium, and minimum opening conditions. Under maximum opening conditions, the target VWAT was set below 24.0 °C. All three designs achieved this target, with the Radial configuration recording the lowest temperature of 23.59 °C, followed by the Butterfly and Iris designs at 23.65 °C and 23.74 °C, respectively. These results indicate that all configurations promoted effective airflow and enhanced cooling performance in fully open conditions.

For medium opening conditions, the target VWAT was 24.0 °C, which is considered optimal for indoor thermal comfort. The Iris design performed closest to this target with a VWAT of 24.02 °C, suggesting near-ideal thermal regulation. The Butterfly design recorded a slightly lower VWAT of 23.86 °C, while the Radial design measured 23.93 °C—both below the target but less precise in achieving the desired thermal comfort level compared to the Iris design. At minimum opening conditions, the target VWAT was above 24.5 °C. The Radial design achieved the highest temperature of 24.71 °C, followed closely by the Iris design at 24.63 °C, both exceeding the target. This suggests that the Radial design is particularly effective in maintaining higher temperatures when airflow is highly restricted. In contrast, the Butterfly design did not meet the 24.5 °C threshold, indicating reduced effectiveness under restrictive conditions.

Fig. 8 *Comparison of the VWAT for Iris, Butterfly, and Radial dampers under various opening conditions*

Quantitative comparison of VWAT values revealed marginal temperature differences (<1%) among the three damper designs. Under maximum and medium opening conditions, the Iris damper recorded temperatures marginally higher than the Butterfly and Radial designs (0.38% and 0.64% slightly warmer), reflecting comparable but slightly reduced cooling efficiency. However, the Iris configuration achieved the closest alignment with the target thermal comfort temperature (24 °C) at medium opening, indicating superior control capability. Under minimum opening conditions, the Iris damper performed marginally better than the Radial design (+0.32% cooler), suggesting enhanced stability under restricted airflow scenarios. Overall, the percentage differences indicate that all designs exhibit nearly equivalent thermal efficiency, with the Iris damper offering the most consistent thermal regulation across operating conditions.

3.2 Volume-weighted Average Velocity Magnitude (VWA*v*)

When selecting a damper design for precision control systems particularly in environments requiring fine regulation of air temperature via controlled airflow. It is essential to evaluate performance across different opening conditions. Ideally, a damper should permit maximal airflow for rapid cooling at full opening and progressively reduce airflow as it closes to facilitate a controlled temperature increase. To characterise airflow behaviour, the VWA*v* was analysed, representing the mean fluid velocity within the computational domain and indicating each design's influence on airflow. Fig. 9 compares VWA*v* for the Iris, Butterfly, and Radial designs under maximum, medium, and minimum openings.

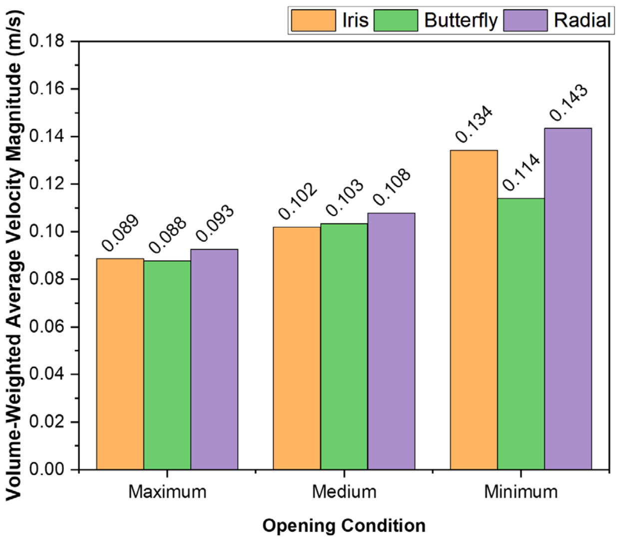

Fig. 9 *Comparison of the VWAv for Iris, Butterfly, and Radial dampers under various opening conditions*

At maximum opening, the Radial damper achieved the highest VWA*v* (0.093 m/s), outperforming the Iris (0.089 m/s) and Butterfly (0.088 m/s) designs by 4.48% and 5.62%, respectively. This suggests that the Radial design is most effective for applications requiring rapid cooling. At medium opening, all designs exhibited higher VWA*v* than at maximum opening, with percentage increases of 14.07% (Iris), 16.41% (Butterfly), and 15.16% (Radial). The Radial maintained the highest velocity, potentially necessitating finer control to avoid excessive cooling. Velocity differences between the Iris and Butterfly relative to the Radial averaged only 4.96%, an acceptable margin for most applications. The lower velocity of the Iris design suggests a gentler airflow, which may reduce the risk of occupant discomfort due to drafts.

At minimum opening, airflow velocities further increased for all designs, consistent with the strategy of limiting airflow to raise temperature. The Radial design again recorded the highest velocity, which could be less desirable for applications demanding minimal airflow. The Iris and Butterfly designs exhibited smaller velocity increases, potentially offering better thermal control under restricted conditions. In summary, the Radial design is optimal for maximum airflow scenarios but may require more sophisticated control strategies at reduced openings. The Iris design offers a balanced performance across conditions, while the Butterfly design's lower velocity increase at minimal opening may be advantageous for systems prioritising temperature maintenance over airflow.

3.3 Volume-weighted Average Static Pressure (VWAP)

The VWAP is a key indicator of the force exerted by the fluid on surfaces, providing insight into how damper design influences the pressure field within the flow. Fig. 10 presents a comparison of VWAP values for the Iris, Butterfly, and Radial designs under maximum, medium, and minimum opening conditions.

At maximum opening, the static pressures were similar among the designs, with the Radial damper recording the highest VWAP (0.844 Pa). This indicates that even when fully open, the Radial design imposes slightly greater airflow resistance, potentially reducing energy efficiency in systems aiming to maintain high flow rates with minimal pressure loss. Under medium opening conditions, the Radial design exhibited a marked pressure increase, reaching 0.930 Pa, compared with 0.844 Pa for the Iris and 0.849 Pa for the Butterfly design. This suggests that the Radial design experiences higher pressure drops during partial closure, which could lead to elevated energy costs in applications requiring precise airflow control. At minimum opening, the Iris design produced the highest VWAP (0.964 Pa), indicating superior sealing performance and potentially greater suitability for scenarios demanding minimal leakage and strict airflow restriction. In contrast, the Butterfly and Radial designs maintained lower pressures, which may allow more airflow under restricted conditions, beneficial for reducing resistance and energy use but less effective for precise airflow limitation.

In summary, an efficient diffuser damper should manage airflow without incurring high static pressures, as lower resistance generally corresponds to reduced energy consumption and quieter operation. The Iris design demonstrated a consistent and progressive pressure increase with closure, making it well-suited for precision control systems. The Radial design, while effective at high airflow, exhibited elevated pressures even at wider openings, which may compromise energy efficiency. The Butterfly design maintained moderate and stable pressure changes, offering a balanced option for applications where extreme precision is unnecessary but moderate control and efficiency are desired

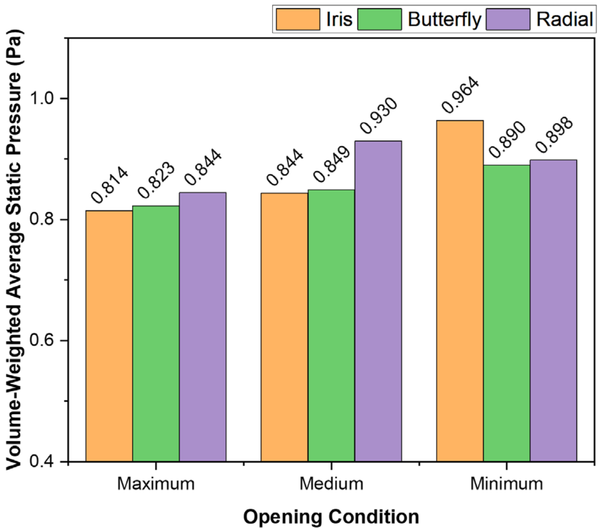

Fig. 10 *Comparison of the VWAP for Iris, Butterfly, and Radial dampers under various opening conditions*

3.4 Volume-weighted Average Turbulent Kinetic Energy (VWA*k*)

Turbulent kinetic energy quantifies the energy contained in turbulent eddies and fluctuations, providing a measure of overall turbulence intensity in the system. It is a key indicator for assessing mixing efficiency, heat transfer potential, and turbulent flow behaviour which are factors that influence both thermal comfort and energy consumption. Fig. 11 compares the VWA*k* for the Iris, Butterfly, and Radial damper designs under maximum, medium, and minimum opening conditions.

At maximum opening, all designs exhibited relatively low VWAk, indicating minimal turbulence as air passed through the dampers. The Radial design recorded the highest value (1.242×10^{-3} m^2/s^2), suggesting greater turbulence generation even in fully open conditions, which could reduce airflow efficiency and increase noise levels. The Iris and Butterfly designs showed slightly lower turbulence, implying smoother airflow. When adjusted to medium opening, VWAk increased for all designs due to the reduced inlet area and associated flow constriction. The Radial design maintained the highest value (1.711×10^{-3} m^2/s^2), followed by the Butterfly (1.519×10^{-3} m^2/s^2) and Iris (1.394×10^{-3} m^2/s^2) designs. The notable increase in the Butterfly design's VWAk suggests a shift in airflow patterns, likely influenced by blade geometry and the resulting flow separation.

At minimum opening, turbulence levels rose further, as expected, with the Radial design reaching a significantly higher VWAk (3.301×10^{-3} m^2/s^2) which is 57.65% greater than the Butterfly and 29.53% greater than the Iris design. This indicates substantial airflow disruption and potential energy inefficiency. While the Iris design's VWAk also increased, it remained lower than the Radial's and slightly above the Butterfly's, suggesting better turbulence control.

Overall, higher turbulent kinetic energy levels correlate with increased energy demand, as HVAC systems must overcome greater resistance in turbulent flows. From an energy efficiency standpoint, dampers with lower turbulent kinetic energy at equivalent opening conditions are preferable. The Iris design demonstrated consistently lower turbulence, particularly at maximum and medium openings, making it the most suitable option for applications prioritising both efficiency and occupant comfort.

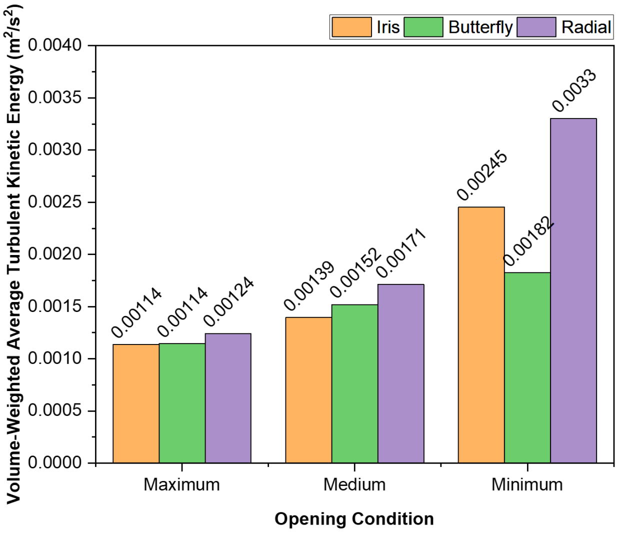

Fig. 11 *Comparison of the VWAk for Iris, Butterfly, and Radial dampers under various opening conditions*

3.5 Volume-Weighted Average Turbulent Intensity (VWATI)

Turbulent intensity is a dimensionless parameter defined as the ratio of the root-mean-square velocity fluctuations to the mean flow velocity. The VWATI provides a domain-wide normalised measure of turbulence, useful for validating turbulence models and predicting noise, vibration, and other factors affecting system design and occupant comfort. Fig. 12 compares the VWATI for the Iris, Butterfly, and Radial damper designs under maximum, medium, and minimum opening conditions.

At maximum opening, all designs exhibited low turbulent intensities, indicating efficient airflow with minimal disturbance. The Iris and Butterfly designs both recorded VWATI values of 2.43%, while the Radial design was slightly higher at 2.53%, suggesting a marginal increase in turbulence generation that could influence noise levels and long-term wear on components. Transitioning from maximum to medium opening resulted in increased VWATI for all designs due to reduced passage area. The Radial design experienced the largest increase (14.78%), indicating greater turbulence generation during partial closure. In comparison, the Iris and Butterfly designs recorded smaller increments of 5.63% and 9.75%, respectively, suggesting more stable and streamlined airflow during intermediate operation.

At minimum opening, turbulence intensified across all designs, with the Radial design reaching the highest VWATI (4.14%), followed by the Iris (3.28%) and Butterfly (2.96%) designs. The elevated turbulence in the Radial design suggests significant airflow disruption, which may negatively impact system efficiency and comfort due to noise and drafts. Despite the overall increase, the Iris design maintained a lower VWATI than the Radial design, indicating better control over turbulence even at near-closed positions.

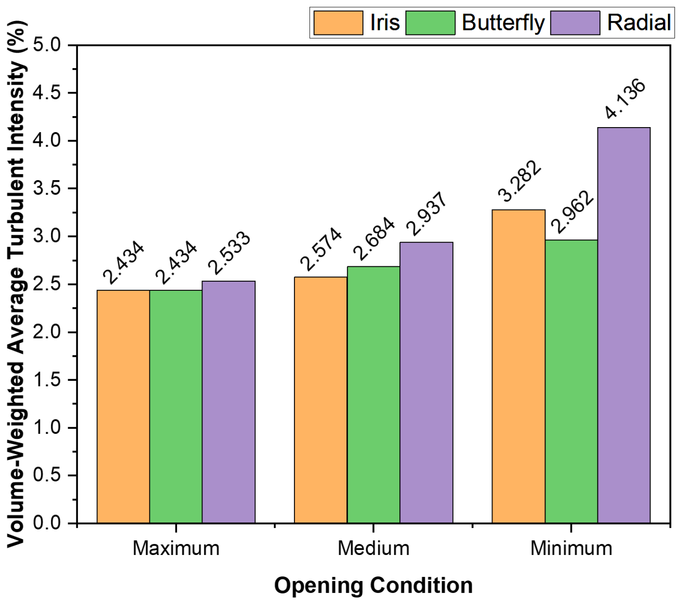

Fig. 12 *Comparison of the VWATI for Iris, Butterfly, and Radial dampers under various opening conditions*

In summary, the Iris design demonstrated consistently lower and more controlled turbulent intensity increases across all opening conditions, making it best suited for precision-controlled, efficiency-focused environments. The Radial design, while capable of delivering high airflow, generated higher turbulence, making it more appropriate for robust, less sensitive applications. The Butterfly design offered a balanced compromise, suitable for general commercial use where moderate noise and energy trade-offs are acceptable.

3.6 Volume-Weighted Average Turbulent Dissipation Rate (VWAε)

Turbulent dissipation rate represents the rate at which turbulent kinetic energy is converted into thermal energy through viscous effects, reducing its capacity to sustain turbulence. In this study, a realizable k–ε turbulence model was applied. The VWAε was used to evaluate turbulence decay across the computational domain, providing insight into eddy lifespan and the tendency of the flow to transition toward a laminar state. Fig. 13 compares VWAε for the Iris, Butterfly, and Radial designs under maximum, medium, and minimum opening conditions.

At maximum opening, VWAε values were the lowest for all designs, indicating minimal conversion of kinetic energy to heat and, thus, more efficient airflow. The Radial design recorded the highest dissipation rate (0.005 m^2/s^3), suggesting greater turbulence generation or higher flow resistance even at full opening. When reduced to medium opening, all designs exhibited a marked increase in VWAε. The Butterfly design showed the largest percentage increase (115.53%), indicating greater sensitivity to partial closure and potentially more significant airflow disruption caused by its blade geometry. The Iris and Radial designs increased by 90.14% and 79.66%, respectively, reflecting less abrupt turbulence changes than the Butterfly design.

At minimum opening, VWAε values rose sharply across all designs, reflecting substantial airflow restriction. The Radial design reached the highest dissipation rate (0.033 m^2/s^3), followed by the Iris (0.030 m^2/s^3) and Butterfly (0.026 m^2/s^3) designs. The elevated dissipation in the Radial design suggests inefficient airflow and higher energy demands for maintaining ventilation, while the Butterfly design's lower value implies reduced turbulence but potentially less restrictive sealing performance.

In summary, higher VWAε indicates increased energy expenditure to maintain airflow against turbulence, reducing system efficiency. The Iris design demonstrated relatively lower dissipation rates under less restrictive conditions, supporting better energy performance in light-to-moderate operation. The Butterfly design's large turbulence shift at medium openings could hinder precise airflow control, while the Radial design's consistently high dissipation rates may limit its suitability in noise-sensitive or comfort-critical environments.

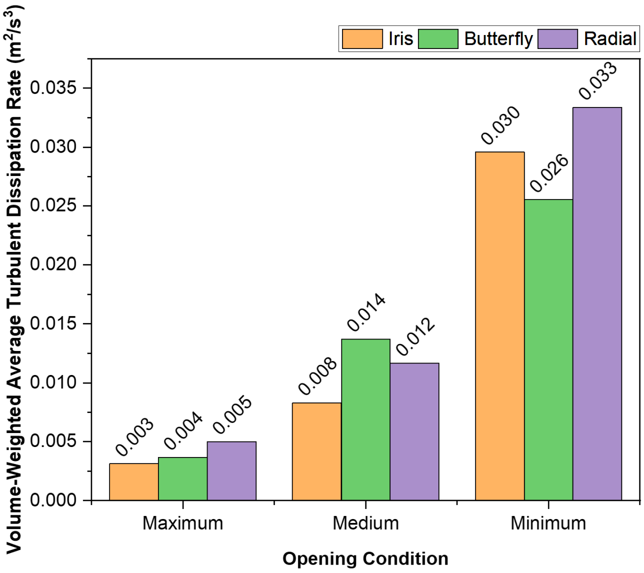

Fig. 13 *Comparison of the VWAε for Iris, Butterfly, and Radial dampers under various opening conditions*

3.7 Temperature Contour Analysis

Table 4 illustrates the static temperature contours for the three damper configurations under maximum, medium, and minimum opening conditions. The contours span from 23.00°C to 24.50°C, capturing both the optimal temperature range and zones of thermal concentration that reflect airflow mixing behavior. Under maximum opening conditions, the Iris damper demonstrated a highly uniform and efficient temperature distribution. The temperature field exhibited lower values concentrated at the diffuser core, gradually increasing toward the periphery. This smooth gradient signifies balanced airflow dispersion and effective thermal mixing, minimizing local temperature deviations. The Butterfly damper also produced a reasonably uniform distribution, though minor variations indicated the presence of localized turbulence. The temperature gradients were less distinct than those of the Iris damper, suggesting moderate mixing efficiency. Nonetheless, the flow field remained largely consistent, supporting acceptable levels of thermal uniformity. In contrast, the Radial damper revealed the least efficient performance, with pronounced spatial temperature variations and clear evidence of uneven mixing. The coexistence of hot and cold zones implied strong turbulence and poor thermal homogeneity, resulting in an overall inefficient temperature field.

At medium opening conditions, the Iris damper maintained a balanced temperature distribution, with a dominant green region surrounded by red, reflecting effective air circulation and thermal mixing within the chamber. A localized hot spot appeared near the lower boundary, likely due to reduced convective exchange in that region. The Butterfly damper exhibited moderate uniformity, with green regions enclosed by warmer orange and red zones, indicating the onset of uneven mixing and intermittent turbulence. Meanwhile, the Radial damper continued to display the most irregular temperature contours, with strong gradients and high thermal stratification. These patterns suggest restricted air movement and incomplete mixing, which reduce the system's ability to sustain consistent comfort conditions.

Under minimum opening conditions, the Radial damper recorded the highest overall temperatures, followed by the Iris damper, both showing extensive red regions corresponding to approximately 24.50°C. Although the Iris configuration exhibited elevated central temperatures, these appeared more localized, implying effective but spatially limited control of airflow and heat dispersion. The Butterfly damper, in contrast, produced the most stable and evenly distributed temperature field, characterized by yellow–orange contours around 24.00°C. This indicates relatively steady airflow and consistent temperature regulation, reflecting superior overall thermal management under restricted flow conditions.

Collectively, these observations reveal that the Iris damper performs optimally at larger openings due to its capacity for balanced airflow distribution and effective mixing, whereas the Butterfly damper maintains good uniformity at smaller openings. Conversely, the Radial damper consistently exhibits significant turbulence and poor thermal uniformity across all operating conditions, underscoring its inefficiency in maintaining stable temperature fields.

Table 4 *The comparison of temperature contour for Iris, Radial and Butterfly damper design*

Damper design	Damper opening condition			Legend
	Maximum	Medium	Minimum	
Iris	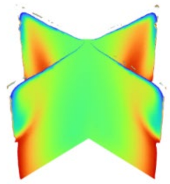	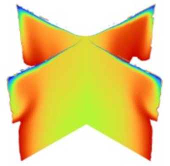		
Butterfly	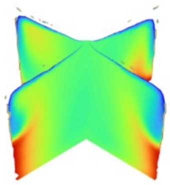	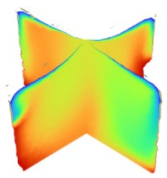	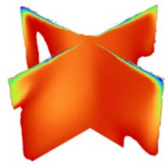	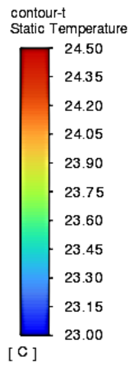
Radial	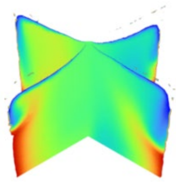	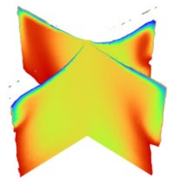		

3.8 Velocity Contour Analysis

Table 5 illustrates the velocity magnitude contours for the Iris, Butterfly, and Radial damper designs under maximum, medium, and minimum opening conditions. The contour range extends from 0.00 m/s to 0.20 m/s, representing the distribution and intensity of airflow across the diffuser domain. These contours provide insights into flow uniformity, turbulence intensity, and the aerodynamic efficiency of each configuration.

Under maximum opening conditions, the Iris damper produced the most uniform velocity distribution, with moderate flow concentrated at the center and smooth diffusion toward the periphery. The absence of sharp gradients indicates minimal recirculation zones and stable flow behavior, signifying efficient momentum transfer and balanced airflow dispersion. The Butterfly damper also exhibited a relatively even velocity field, although minor irregularities were observed near the boundaries, possibly due to asymmetrical vane interactions. These features suggest partial turbulence and secondary flow formations but without significantly disrupting overall flow uniformity. In contrast, the Radial damper displayed highly non-uniform contours, characterized by distinct high-velocity jets and localized low-velocity pockets. Such irregular patterns are indicative of flow separation and energy losses, which reduce aerodynamic efficiency and contribute to uneven air distribution within the conditioned space.

At medium opening conditions, the Iris damper maintained stable flow characteristics, with consistent velocity gradients radiating from the center. This behavior suggests efficient mixing and controlled jet dispersion, supporting balanced airflow even under partial restriction. The Butterfly damper revealed moderate velocity uniformity with noticeable high-velocity streaks extending toward the corners, indicating turbulence amplification due to partial blade obstruction. The Radial damper, however, demonstrated strong fluctuations in velocity magnitude, with pronounced high-speed regions near the outlets and low-speed recirculation near the central area. This pattern confirms unstable flow behavior and inadequate directional control, leading to poor air delivery uniformity.

Under minimum opening conditions, all designs exhibited reduced overall velocity magnitudes; however, their flow characteristics varied substantially. The Butterfly damper achieved the most consistent velocity field, maintaining moderate flow strength and minimizing stagnant zones. This suggests superior adaptability to low-flow conditions, where controlled restriction promotes even dispersion. The Iris damper showed localized high-velocity cores near the diffuser center, indicating concentrated jets and reduced peripheral mixing. Conversely, the Radial damper produced the most turbulent and uneven velocity field, dominated by strong gradients and recirculation pockets. These features point to high energy dissipation and poor flow directionality, resulting in suboptimal ventilation performance at restricted openings.

Overall, the velocity contour analysis confirms that the Iris damper performs best under high-flow conditions due to its symmetrical flow guidance and efficient distribution. The Butterfly damper demonstrates versatility and maintains acceptable uniformity across all operating states, particularly at lower openings. Meanwhile, the Radial damper consistently exhibits inferior aerodynamic behavior, with pronounced turbulence, flow separation, and poor mixing efficiency across all opening conditions.

Table 5 *The comparison of velocity contour for Iris, Radial and Butterfly damper design*

Damper design	Damper opening condition			Legend
	Maximum	Medium	Minimum	
Iris	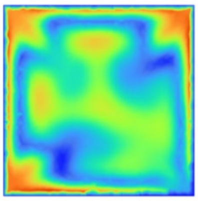	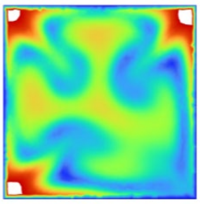	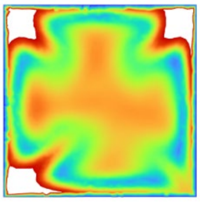	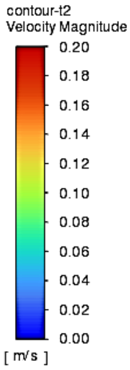
Butterfly	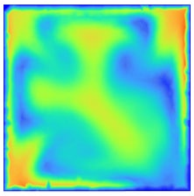	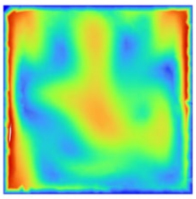	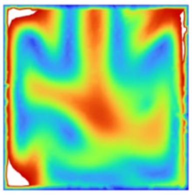	
Radial	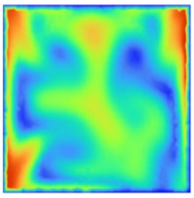	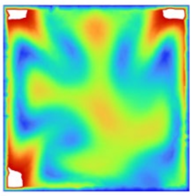	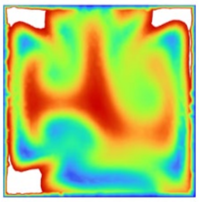	

3.9 The Performance Evaluation Summary

The Iris design emerged as the most effective option across all evaluated performance metrics. It provided precise airflow regulation, consistently maintained lower turbulence and turbulent intensity levels, and delivered smooth, stable airflow. Additionally, it demonstrated excellent temperature control, making it highly suitable for applications requiring precise thermal regulation and gradual airflow transitions, thereby ensuring both occupant comfort and energy efficiency. The Butterfly design ranked second, offering good overall control. It maintained moderate velocity changes and effective temperature regulation across various openings, delivering balanced and predictable performance. While less precise than the Iris design, its stability and gradual modulation made it well-suited for general comfort applications where extreme precision was not essential but consistent environmental conditions were important.

The Radial design, although efficient in certain scenarios, such as achieving high airflow velocities and sustaining higher temperatures at minimal openings but was less suitable for general indoor comfort. Its aggressive airflow modulation and elevated turbulence levels at reduced openings limited its suitability for precise environmental control. However, it remains a viable choice for specialised applications prioritising robust airflow over gradual modulation. Overall, the Iris design was selected as the optimal choice for most HVAC systems. Its combination of efficient, controlled airflow; reduced turbulence; and lower static pressure levels makes it ideal for enhancing thermal comfort and improving energy efficiency. In summary, the Iris damper offers the most comprehensive performance for precise and efficient control, suitable for a wide range of indoor environments.

4. Conclusions

This study comprehensively evaluated the airflow and thermal performance of three diffuser damper designs, Iris, Butterfly, and Radial, under varying opening conditions using VWA analysis. The results consistently showed that the Iris damper achieved more stable and uniform airflow, reduced turbulence intensity, and improved temperature distribution compared to the other configurations.

Beyond these numerical outcomes, the findings carry practical implications for HVAC system design and operation. The ability of the Iris damper to maintain controlled and evenly distributed airflow suggests potential for reduced fan energy demand, lower pressure losses, and enhanced thermal comfort uniformity in occupied spaces. Such characteristics can contribute to improved overall energy efficiency and more effective zone-level environmental control.

Therefore, based on both performance metrics and design implications, the Iris damper can be recommended as the optimal configuration for HVAC systems that prioritize energy-efficient air distribution, occupant comfort, and operational stability across varying load conditions.

Acknowledgement

The authors would like to thank Universiti Tun Hussein Onn Malaysia (UTHM) for the full support of the research work. This work was financially supported by the TIER 1 Grant Scheme Vot No. Q394. The authors would like to thank Universiti Teknologi Malaysia (UTM) for the support of the research work.

Conflict of Interest

Authors declare that there is no conflict of interests regarding the publication of the paper.

Author Contribution

The authors confirm contribution to the paper as follows: ***study conception and design:*** *Nur'Amirah Busu, Norasikin Mat Isa;* ***data collection:*** *Nur'Amirah Busu;* ***analysis and interpretation of results:*** *Nur'Amirah Busu, Norasikin Mat Isa;* ***draft manuscript preparation:*** *Nur'Amirah Busu;* ***technical advice****: M.F. Abdul Gani. All authors reviewed the results and approved the final version of the manuscript.*

References

[1] Yuanzheng Li, Wenjing Wang, Yating Wang, Yashu Xin, Tian He & Guosong Zhao (2021) A review of studies involving the effects of climate change on the energy consumption for building heating and cooling. *International Journal of Environmental Research and Public Health*, *18(1)*, 40, https://doi.org/10.3390/ijerph18010040

[2] Jeffrey Leong (2023) Computational Fluid Dynamics (CFD) Study on air flow of air diffuser in a room, *Research Progress in Mechanical and Manufacturing Engineering*, *4(1)*, 365-378, https://penerbit.uthm.edu.my/periodicals/index.php/rpmme/article/view/9288/3973

[3] Essam E. Khalil, Gamal ElHariri, Eslam Abdelghany & Mahmoud AbouSaad (2021) Numerical investigation of flow patterns and thermal comfort inside air-conditioned square diffuser in teaching space. In *AIAA Scitech 2021 Forum* (p. 1983), https://doi.org/10.2514/6.2021-1983

[4] Omer E. Mohamed, Amr Ahmed & Musa Abubker (2024, June 16-18). *CFD of the conditioned air distribution in a hospital operating room* [In Proceedings of the 11th International Conference on Fluid Flow, Heat and Mass Transfer (FFHMT 2024) Chestnut Conference Centre], Toronto, Canada. https://doi.org/10.11159/ffhmt24.040

[5] Omer E. Mohamed, Amr Ahmed & Musa Abubker (2024) CFD of Human Comfort and Contaminants Control in a Hospital Operating Room, *Journal of Fluid Flow, Heat and Mass Transfer Учредители: Avestia Publishing*, *11*, 286-295, https://doi.org/10.11159/jffhmt.2024.029

[6] Joanna Maria Kopania, Grzegorz Bogusławski, Kamil Wójciak & Patryk Gaj (2024) The noise study of ceiling swirl diffuser with serrated adjustable blades, *Vibrations in Physical Systems*, *35(2)*, 1-8, http://doi.org/10.21008/j.0860-6897.2024.2.02

[7] Mengchao Liu, Ran Gao, Yujiao Zhao & Angui Li (2025), Swirl diffuser shape optimization based on a comprehensive evaluation index for both winter and summer conditions, *Indoor and Built Environment*, *34(4)*, 736-750, https://doi.org/10.1177/1420326X251319479

[8] Linye Song, Kaijun Li, Xinghui Zhang & Jing Hua (2024) An active diffuser control method based on the constant jet throw for improving airflow distribution in variable air volume systems, *Indoor and Built Environment*, *33(1)*, 74-94, https://doi.org/10.1177/1420326X231184629

[9] Dong Yoon Park, & Seongju Chang (2020) Effects of combined central air conditioning diffusers and window-integrated ventilation system on indoor air quality and thermal comfort in an office, *Sustainable Cities and Society*, *61*, 102292, https://doi.org/10.1016/j.scs.2020.102292

[10] Farrokh Jazizadeh, Vedant Joshi & Francine Battaglia (2020) Adaptive and distributed operation of HVAC systems: Energy and comfort implications of active diffusers as new adaptation capacities, *Building and Environment*, *186*, 107089, https://doi.org/10.1016/j.buildenv.2020.107089

[11] Yuxin Wu, Panu Mustakallio, Risto Kosonen, Tuomas Kaukola, Jingdong Chen, Hong Liu & Baizhan Li (2022) Experimental study of five different VAV air terminal devices under variable heat gain conditions in simulated office and meeting rooms, *Building and Environment*, *209*, 108641, https://doi.org/10.1016/j.buildenv.2021.108641

[12] Shanrui Shi, Shohei Miyata, Yasunori Akashi, Masashi Momota & Takao Sawachi (2023, September 4-6). *Neutralizing room pressure in multi-room VAV systems through model-based static pressure reset control* [In Building Simulation 2023: 18th Conference of IBPSA], Shanghai, China, (Vol. 18, pp. 3231-3238), https://doi.org/10.26868/25222708.2023.1293

[13] Hao Wan-Jun, Qiao Yan-Hui, Song Lu-Lu, Liu Jing-Lin, Fan Rong, Liu Meng-Xue & Chen Lin (2016, May 28-30). *A fuzzy control strategy with enhanced robustness for VAV systems considering fan model uncertainties* [In 2016 Chinese Control and Decision Conference (CCDC)] IEEE, Yinchuan, China, pp. 6292-6296, https://doi.org/10.1109/CCDC.2016.7532130

[14] Yuanpeng Mu, Jili Zhang, Zhixian Ma, and Mingsheng Liu (2023) A novel air flowrate control method based on terminal damper opening prediction in multi-zone VAV system, *Energy*, *263*, 126031, https://doi.org/10.1016/j.energy.2022.126031

[15] Hao Wang, Xiwen Chen, Natan Vital, Edward Duffy & Abolfazl Razi (2024) Energy optimization for HVAC systems in multi-VAV open offices: A deep reinforcement learning approach, *Applied Energy*, *356*, 122354, https://doi.org/10.1016/j.apenergy.2023.122354

[16] Xu Zhu, Taotao Shi, Xinqiao Jin & Zhimin Du (2021) Multi-sensor information fusion based control for VAV systems using thermal comfort constraints. *Building Simulation*, *14(4)*, 1047-1062, https://doi.org/10.1007/s12273-020-0736-9

[17] Shanrui Shi, Shohei Miyata, Yasunori Akashi, Masashi Momota, Takao Sawachi & Yuan Gao (2024) Model-based optimal control strategy for multizone VAV air-conditioning systems for neutralizing room pressure and minimizing fan energy consumption, *Building and Environment*, *256*, 111464, https://doi.org/10.1016/j.buildenv.2024.111464

[18] Nabil Nassif, Mostafa Tahmasebi, Iffat Ridwana & Pejman Ebrahimi (2022) New optimal supply air temperature and minimum zone air flow resetting strategies for VAV Systems, *Buildings*, *12(3)*, 348, https://doi.org/10.3390/buildings12030348

[19] Nur'Amirah Busu, Norasikin Mat Isa, Azian Hariri & Mohamed Hussein (2022) An experimental study of real-time temperature distribution using iris damper without control system: A justification analysis, *Journal of Advanced Research in Technology and Innovation Management*, *4(1)*, 24-31, https://doi.org/10.37934/jartim.4.1.2431

[20] N. Busu, Isan Mat, A. Hariri, M. Hussein & D. Adebayo (2024) Exploring the effect of indoor thermal comfort using Iris dampers: A justification study, *Journal of Advanced Research*, *121(2)*, 1-11, https://doi.org/10.37934/arfmts.121.2.111

[21] Nur'Amirah Busu, Norasikin Mat Isa, Azian Hariri & Mohamed Hussein (2024, February 27-29). *Revolutionizing indoor thermal comfort: Iris damper integration with step-based control in central air conditioning system* [In 2024 2nd International Conference on Mechatronics, Control and Robotics (ICMCR)], IEEE, Jeju, Republic of Korea, pp. 62-66, https://doi.org/10.1109/ICMCR60777.2024.10482191

[22] M. H. Irfan, N. M. Isa, N. A. Busu, A. Hariri, M. Amirul & M. Hussein (2024) Investigation of airflow patterns and thermal efficiency in different ducting configurations by using CFD. *International Journal of Mechanical and Sustainability Engineering Technology*, *1*, 46-56.

[23] N. Busu, Norasikin Mat Isa, Azian Hariri & Mohamed Hussein (2023) The comparison of P, PI and PID strategy performance as temperature controller in active iris damper for centralized air conditioning system, *Journal of Advanced Research in Fluid Mechanics and Thermal Sciences*, *102(2)*, 143-154, https://doi.org/10.37934/arfmts.102.2.143154

[24] Ran Gao, Shihao Wen, Angui Li, Hengchun Zhang, Wuyi Du & Baoshun Deng (2019) A novel low-resistance damper for use within a ventilation and air conditioning system based on the control of energy dissipation, *Building and environment*, *157*, 205-214, https://doi.org/10.1016/j.buildenv.2019.04.041

[25] Dong Yoon Park & Seongju Chang (2020) Effects of combined central air conditioning diffusers and window-integrated ventilation system on indoor air quality and thermal comfort in an office, *Sustainable Cities and Society*, *61*, 102292, https://doi.org/10.1016/j.scs.2020.102292

[26] Brijesh Pandey, Rangan Banerjee & Atul Sharma (2021) Coupled EnergyPlus and CFD analysis of PCM for thermal management of buildings, *Energy and Buildings*, *231*, 110598, https://doi.org/10.1016/j.enbuild.2020.110598